Supporting Information

Kozmik *et al*. 10.1073/pnas.0800388105

Materials and Methods

Jellyfish Collection and Culture. Adult *Tripedalia cystophora* were collected in mangroves of La Parguerra, Puerto Rico. Laboratory cultures were established using settling larvae and artificial sea water. Settled larvae metamorphosed into young polyps. Young polyps were transformed into budding (asexually reproducing) polyps by feeding with artemia once a week. Spontaneously metamorphosed polyps (newborn medusae) were fixed for *in situ* hybridization. Polyps as well as young medusae were maintained at 26°C.

Isolation of Rhopalium-Expressed Genes. The expressed sequence tag (EST) cDNA library was generated from rhopalia mRNA by using pBluescript II. Individual clones from the library were sequenced using an ABI capillary sequencer, and full-length cDNAs were obtained by SMART RACE (BD Biosciences). A fragment of *Tripedalia* Mitf cDNA was isolated by reverse transcription-PCR of rhopalia mRNA by using degenerate primers zk665A 5′-AARAARGAYAAYCAYAA-3′ and zk665F 5′-TTDATNCKRTCRTTDATRTT-3′. The resulting partial Mitf cDNA was extended by RACE. The accession numbers for the clones are as follows: *c-opsin* (EU310498), *oca* (EU310502), *mitf* (EU310499), catalytic *pde* (EU310500), inhibitory *pde6d* (EU310501), and guanylate cyclase (EU310503).

Phylogenetic Analysis. Amino acid alignment created by MUSCLE software (11) with default settings was edited manually, and highly divergent stretches were excluded. The phylogenetic trees were constructed using the Phylip 3.6 package. Bootstrap sample set was generated by SEQBOOT (1,000 replicates), protein distances were estimated using PROTDIST (PAM matrix, 1,000 datasets), and the NJ tree was constructed by NEIGHBOR (1,000 replicates, random input order) and CONSENSE programs. Maximum-likelihood trees were constructed by PROML (JTT matrix, random input order, 500 replicates) and final consensus tree by CONSENSE. The numbers above each node represent the percentage of bootstrap probability based on 1,000 replicates. *Tripedalia* protein sequences clustered consistently in trees inferred by the maximum-likelihood method. Accession numbers of sequences used in the trees are as follows.

Opsin tree. The numbers of *Strongylocentrotus purpuratus* genes represent the gene ID in public assembly of Sea Urchin Genome Project (hgsc.bcm.tmc.edu/projects/seaurchin), Gallus adenosine receptor NP_990418.1, *Mus* serotonine receptor NP_766400.1, *Branchiostoma belcheri* opsin 6 BAC76024.1, *Drosophila* Rh6 NP_524368.3, *Drosophila* Rh2 NP_524398.1, *Drosophila* Rh3 NP_524411.1, *Apis* blue rhodopsin NP_001011606.1, *Octopus* opsin P09241, *Sepia* rhodopsin AAC26329.1, *Mizuhopecten* Gq O15973, *Platynereis* r-opsin CAC86665.1, *B. belcheri* Mop Q4R1I4, *Xenopus* melanopsin AAC41235.1, *Danio* melanopsin NP_840074.1, *Homo* melanopsin NP_150598.1, *Danio* LW NP_571250.1, *Homo* MW NP_000504.1, *Gallus* LW NP_990740.1, *Homo* rhodopsin NP_000530.1, *Danio* extraocular NP_571287.1, *Danio* MW4 NP_571329.1, *Latimeria* Rh2 AAD30520.1, *Danio* SW opsin NP_571394.1, *Xenopus* violet P51473, *Xenopus* green AAO38746.1 *Gallus* blue NP_990848.1, *Salmo* VAL opsin O13018, *Danio* VAL opsin NP_571661.1, *Ciona* opsin NP_001027727.1, *Xenopus* parapinopsin NP_998830.1, *Uta* parietopsin AAZ79904.1, *Xenopus* parietopsin NP_001039256.1, *Mus* encephalopsin NP_034228.1, *Homo* encephalopsin NP_055137.2, *Platynereis* c-opsin AAV63834.1, *Takifugu* TMT NP_001027778.1, *B. belcheri* opsin 4 BAC76021.1, *B. belcheri* opsin 5 BAC76022.1, *Apis* pteropsin NP_001035057.1, *Aedes* opsin EAT43163.1, *Anopheles* GPRop11 XP_312503.3, *Anopheles* GPRop12 XP_312502.2, *Strongylocentrotus* Sp1 GLEAN3_05569, *Mizuhopecten* G_o O15974, *B. belcheri* opsin 2 BAC76020.1, *B. belcheri* opsin 1 BAC76019.1, *Strongylocentrotus* Sp3.2 GLEAN3_27633, *Strongylocentrotus* Sp3.1 GLEAN3_27634, *Rattus* Opn5 NP_861437.1, *Homo* Opn5 NP_859528.1, *Homo* peropsin NP_006574.1, *Mus* peropsin AAC53344.1, *B. belcheri* opsin 3 BAC76023.1, *Gallus* RGR NP_001026387.1, *Mus* RGR NP_067315.1, *Todarodes retinochrome* CAA40422.1.

MITF/TFE tree. *Saccharomyces cerevisiae* RTG3 NP_009447.1, *Caenorhabditis briggsae* XP_001671854.1, *Caenorhabditis elegans* NP_500461.1, *Nematostella vectensis* XP_001636474.1, *Ciona intestinalis* NP_001087207.1, *Apis mellifera* XP_394278.2, *Drosophila melanogaster* AAQ01726.1, *Mus musculus* TfeB NP_035679.2, *Homo sapiens* TfeB NP_009093.1, *M. musculus* Tfe3 NP_766060.2, *H. sapiens* Tfe3 NP_006512.2, *Danio rerio* Tfe3 CAE30419.1, *D. rerio* TfeC CAH68937.1, *H. sapiens* TfeC NP_036384.1, *M. musculus* TfeC NP_112475.1, *D. rerio* MiTF NP_570998.1, *M. musculus* MiTF AAI08978.1, *Canis lupu familiaris* MiTF NP_001003337.1, *H. sapiens* MiTF NP_006713.1, *Xenopus tropicalis* MiTF NP_001093747.1, *Gallus gallus* NP_990360.1.

Catalytic PDE tree. *H. sapiens* PDE1A P54750, *Strongylocentrotous purpuratus* PDE5 NP_001029121.1, *H. sapiens* PDE5A (NP_001074), *D. melanogaster* PDE6 (CG8279-PA) AAF55066, *H. sapiens* PDE1A NP_005010.2; *S. purpuratus* PDE1 NP_001091918.1, *H. sapiens* PDE2A NP_002590.1, *S. cerevisiae* PDE2-like NP_015005.1, *S. cerevisiae* PDE1 CAA64139.1, *H. sapiens* PDE3A NP_000912.3, *Rattus norvegicus* PDE3 (predicted) XP_574187.2, *H. sapiens* PDE4 ANP_006193.1, *D. melanogaster* PDE4 (CG32498) AAF45865.2, *Nematostella vectensis* PDE5 (predicted) XP_001631585.1, *H. sapiens* PDE5A1 NP_001074.2, *D. melanogaster* PDE6 (CG8279-PA) NP_650369.2, *H. sapiens* PDE6A P16499, *H. sapiens* PDE6B P35913, *H. sapiens* PDE6C P51160, *N. vectensis* PDE6-like XP_001636689.1, *H. sapiens* PDE7A NP_002594.1, *M. musculus* PDE7 NP_032828.1, *D. melanogaster* PDE8A AAM68263.1, *H. sapiens* PDE8B NP_003710.1, *D. melanogaster* PDE9 (CG32648-PA) NP_727644.1, *H. sapiens* PDE9A AF048837, *H. sapiens* PDE11A1 NP_001070664.1, *H. sapiens* PDE11A2 NO00107826, *D. melanogaster* PDE11 (CG10231-PA) NP_609885.1, *D. melanogaster* PDE11 XP_001356584.1, *Trichomonas vaginalis* GAF-containing protein (GAF PDE outgroup) XP_001324213.1.

PDE6D alignment. *Nemastostella* PDE6pred XP_001629547.1, *Homo* PDE6D NP_002592.1, *Mus* PDE6D 032827.1, *Bos* PDE6D NP_776845.1, *Canis* PDE6D NP_001003156.1, *Ciona* PDE6D_NP_001027639.1, *Apis* PDE6delta_XP_394004.2, *Strongylocenter* PDE6delta_XP_001177685.1, *Caenorhabditis* PDE6delta_NP_495490.1, *Aedes* PDE6delta XP_320754.1, *Drosophila* GA21678-PA_XP_001355815.1, *Tetrahymena* GMPPDE_XP_001007775.1.

Oca2 tree. *H. sapiens* OCA2 NP_000266.2, *Sus scrofa* OCA2 NP_999259.2; *Oryzias latipes* OCA2 NP_001098262, *M. musculus* OCA2 NP_068679, *G. gallus* OCA2 XP_425579, *Nematostella vectensis* _OCA2XP_001627452, *D. melanogaster* RE09889 (P protein) AAN71295.1, *Aedes aegypti* Tyr transp (hoepl-like) XP_001658764.1, *D. melanogaster* Tyr_transp (hoepl1) NP_608876.1hoepel1, *Clostridium botulinum* Ars pump YP_001253041.1, *Carboxydothermus hydrogenoformans* Ars transp YP_360838.1, *Thermococcus kodakarensis* Ars pump.

Membrane-associated guanylate cyclase tree. *Strognylocentrotus* GC NP_999705.1, *Asterias* GC BAB85468.1, *Xenopus* GC 2C NP_001079334.1, *Mus* GC 2C NP_659504.1, *Homo* GC 2C NP_004954.1, *Xenopus* GC 2B NP_001084176.1, *Anguilla* GC 2B P55202.1, *Homo* GC 2B P20594.1, *Mus* GC 2A P18293.2, *Aedes* retinal -type GC XP_001658332.1, *Mus* GC 2E NP_032218.2, *Homo* GC 2D NP_000171.1, *Bos* GC 2D NP_776973.1, *Canis* GC 2D NP_001003207.1, *Gallus* GC 2E AAC24500.1, *Mus* GC 2D XP_001474460.1, *Oryzias* Olgc-R1 NP_001098133.1, *Danio* GC 2F XP_689630.1, *Oryzias* OlGC5 NP_001098551.1, *Oryzias* OlGC-R2 BAA76301.1, *Danio* GC 2 NP_001103165.1, *Bos* GC 2F NP_776974.1, *Homo* GC 2F NP_001513.2, *Rattus* GC 2F NP_446283.1, *Mus* GC 2F NP_001007577.1. The last 80 amino acids of protein kinase-like domain of guanylate cyclases were aligned. Membrane guanylate cyclase of *Strongylocentrotus* and *Asterias* were used as an outgroup.

Phosducin tree. *Homo* PhLP3 NP_076970.1, *Rattus* PhLP3 NP_001020880.1, *Danio* PhLP3 46391102; *Nematostella* (protein ID) 119091, *Drosophila* AAF49974.2, *Mus* PhLP2 NP_075997.1, *Homo* PhLP2 NP_689614.2, *Bos* PhLP2 NP_001035641.1, *Schizosaccharomyces* CAB39851.2, *Mus* PhL AAH06578.1, *Bos* PhL NP_001035641.1, *Homo* PhL NP_005379.3, *Danio* phosducin AAH60908.1, *Mus* phosducin Q9QW08.1, *Homo* phosducin NP_002588.3, *Canis* phosducin NP_001003076.1. Amino acid sequences spanning from helix 5 up to the end of helix 7 of phosducin protein family were aligned.

Analysis by RT-PCR. Total RNA was isolated from *Tripedalia cystophora* rhopalia using TRIzol reagent (Invitrogen). The RT reaction was performed using random oligonucleotide hexamers in the presence or absence (negative control) of the PowerScript enzyme (Clontech). The specific primers for the phototransduction genes were as follows: *guanylate cyclase*, 5′-GGATGTCTACAGCTATGGCATCAT-3′ (forward) and 5′-CGTTGATTCTTTTCATGACTTTCA-3′ (reverse); inhibitory *PDE6D*, 5′-TCTACCGTTAACGAAATGCAGCAC-3′ (forward) and 5′-GTCTCGTATCAATCTGTACTTTGC-3′ (reverse); catalytic *PDE*, 5′-GAGGACTATTCTCTGCATGCCCAT-3′ (forward) and 5′-GTTCTTCCTGACGGATAAGATCCA-3′ (reverse); *phosducin*, 5′-CCAGCAATATCCACAGATCAA-3′ (forward) and 5′-TCGAATCGGTTTCGCTATTCC-3′ (reverse).

Expression, Reconstitution, and Spectroscopic Analysis of *Tripedalia* c-Opsin. The entire coding region was amplified from the *Tripedalia* c-opsin cDNA clone by primer pairs designed within the 5′ and 3′ edges of the coding regions with necessary sequences for cloning and translation purposes as in ref. 12: 5′-AAAAAA-GAATTCCACCATGGCAGATCACGGAAGGAATAC-3′ (the forward primer with an EcoRI site underlined) and 5′-TTCTAGGTCGACTCCGGCTCAACA-GAATTTCCACAGAG-3′ (the reverse primer with a SalI site underlined). Via the restriction sites set in the primers, the amplified cDNA fragment was cloned into the pMT5 expression vector, which contains the last 15 amino acids of the bovine rod opsin necessary for immunoaffinity purification by 1D4 monoclonal antibody (13). Cultured COS-1 cells (RIKEN Cell Bank) were transfected with the pMT5-cDNA clone, incubated with 5 μM 11-*cis*-retinal (Storm Eye Institute, Medical University of South Carolina, Charleston, SC), and solubilized with 1% dodecyl maltoside. The c-opsin photopigment was purified using immobilized 1D4 (Cell Culture Center, Minneapolis, MN). The UV-visible absorption spectrum was recorded for the c-opsin photopigment from 250 to 650 nm at 0.5-nm intervals using the Hitachi U3010 dual beam spectrometer at 20°C. Five replicates were performed in the dark and five more after 3 min of light exposure (with a $<$440 nm cut-off filter) as described in ref. 13. The Savitzky–Golay least-squares smoothing method was carried out for the absorbance curve, with 100 repetitions to eliminate spurious spikes. The λ_{max} value was taken from the dark–light difference spectrum.

1. Terakita A (2005) The opsins. *Genome Biol* 6:213.
2. Franke RR, Sakmar TP, Graham RM, Khorana HG (1992) Structure and function in rhodopsin: Studies of the interaction between the rhodopsin cytoplasmic domain and transducin. *J Biol Chem* 267:14767–14774.
3. Madabushi S, *et al*. (2004) Evolutionary trace of G protein-coupled receptors reveals clusters of residues that determine global and class-specific functions. *J Biol Chem* 279:8126–8132.
4. Arendt D, Tessmar-Raible K, Snyman H, Dorresteijn AW, Wittbrodt J (2004) Ciliary photoreceptors with a vertebrate-type opsin in an invertebrate brain. *Science* 306:869–871.
5. Florio SK, Prusti RK, Beavo JA (1996) Solubilization of membrane-bound rod phosphodiesterase by the rod phosphodiesterase recombinant delta subunit. *J Biol Chem* 271:24036–24047.
6. Bauer PH, *et al*. (1992) Phosducin is a protein kinase A-regulated G-protein regulator. *Nature* 358:73–76.
7. Sokolov M, *et al*. (2004) Phosducin facilitates light-driven transducin translocation in rod photoreceptors: Evidence from the phosducin knockout mouse. *J Biol Chem* 279:19149–19156.
8. Shyjan AW, de Sauvage FJ, Gillett NA, Goeddel DV, Lowe DG (1992) Molecular cloning of a retina-specific membrane guanylyl cyclase. *Neuron* 9:727–737.
9. Lowe DG, *et al*. (1995) Cloning and expression of a second photoreceptor-specific membrane retina guanylyl cyclase (RetGC), RetGC-2. *Proc Natl Acad Sci USA* 92:5535–5539.
10. Hallsson JH, Haflidadottir BS, Schepsky A, Arnheiter H, Steingrimsson E (2007) Evolutionary sequence comparison of the Mitf gene reveals novel conserved domains. *Pigment Cell Res* 20:185–200.
11. Edgar RC (2004) MUSCLE: Multiple sequence alignment with high accuracy and high throughput. *Nucleic Acids Res* 32:1792–1797.
12. Matsumoto Y, Fukamachi S, Mitani H, Kawamura S (2006) Functional characterization of visual opsin repertoire in Medaka (*Oryzias latipes*). *Gene* 371:268–278.
13. Kawamura S, Yokoyama S (1998) Functional characterization of visual and nonvisual pigments of American chameleon (*Anolis carolinensis*). *Vision Res* 38:37–44.

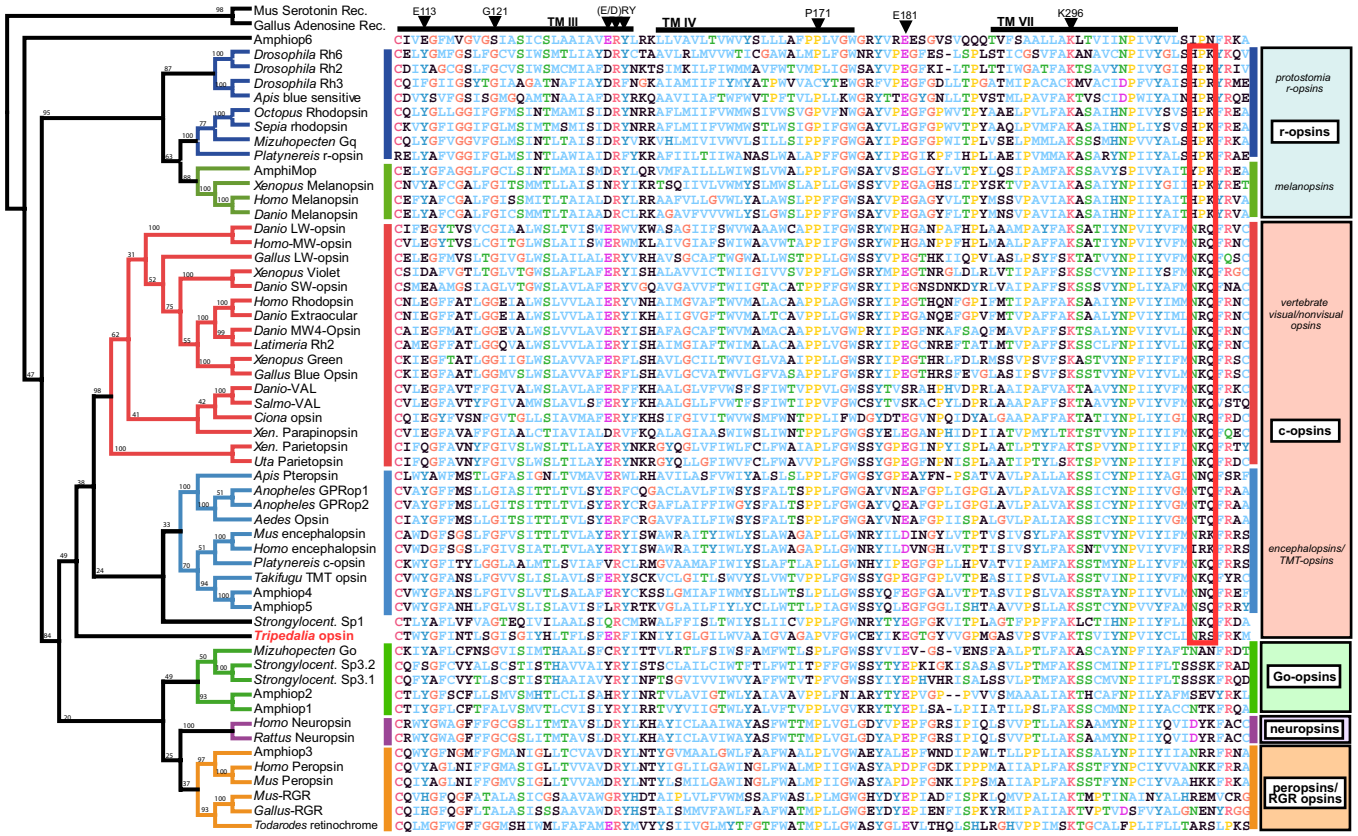

Fig. S1. Alignment and phylogenetic tree of opsins. The phylogenetic tree was inferred by the neighbor-joining method using murine adenosine and chicken serotonin receptors as outgroup sequences. Nonhomologous stretches were excluded from the analysis. The black lines above the alignment represent the extent of transmembrane helices III, IV, and VII. The color lines on both sides of the alignment demarcate opsin subfamilies. Critical amino acids allowing opsin classification are indicated by the black arrowheads and numbered according to the bovine rhodopsin protein sequence. The lysine residue K296 is critical for covalent binding of retinal via Schiff base linkage, which is stabilized by counterion E113 or E181 (1). The (E/D)RY triade, which is highly conserved among G protein-coupled receptors (GPCRs), is important for G protein interaction (2). G121, P171, and W175 are evolutionary trace residues typical for the opsin family but not for the GPCRs in general (3). The positions of the HPK and the NR/KQ motifs conserved among rhabdomeric and ciliary opsins, respectively (4), are boxed in red. The classification of opsin families is given in the colored boxes on the right.

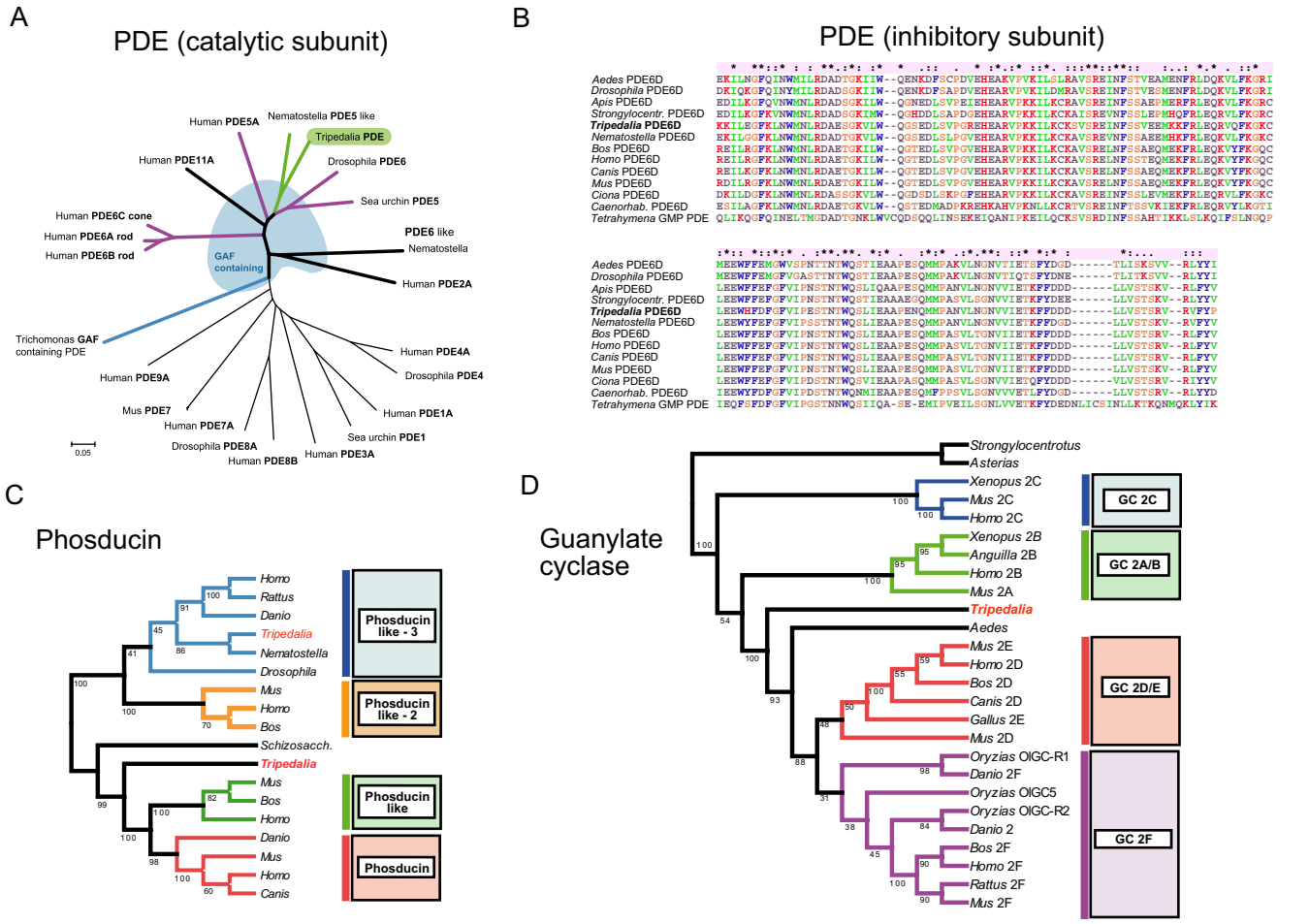

Fig. S2. Phylogenetic analysis of *Tripedalia* components of the ciliary phototransduction cascade. (*A*) Phylogenetic tree of the catalytic subunit of the *phosphodiestrase* (*PDE*) gene family. *Tripedalia* PDE contains two GAF domains and a phosphodiesterase catalytic domain, PDase I. *Tripedalia* PDE groups with cGMP-specific PDEs used in phototransduction and is phylogenetically close to PDE5 and PDE6. (*B*) Alignment of the inhibitory subunit of *phosphodiesterase PDE6D*. A δ subunit of PDE (PDE6D) in the rod outer segment can bind the PDE$\alpha\beta\gamma_2$ complex and solubilize it, disrupting its normally close association with the disk membrane (5). Among bilaterians, the highest degree of sequence identity/similarity of *Tripedalia* PDE6D is with PDE6D from various vertebrates. The percentage of identity/similarity between *Tripedalia* and other species is as follows: *Homo* (82/94%), *Bos* (82/94%), *Canis* (82/95%), *Mus* (81/94%), *Ciona* (80/91%), *Strongylocentrotus* (74/92%), *Caenorhabditis* (69/89%), *Aedes* (62/84%), and *Drosophila* (59/82%). (*C*) Phylogenetic tree of the *phosducin* gene family. Phosducin modulates phototransduction by interacting with the $\beta\gamma$ subunits of G protein transducin (6, 7). *Phosducin* and *phosducin-like* genes are expressed in *Tripedalia*, the former clustering with the vertebrate retina-specific *phosducins*. (*D*) Phylogenetic tree of the *guanylate cyclase* (*GC*) gene family. *Tripedalia* guanylate cyclase clusters with membrane-associated retina-specific GC2E (also known as retGC-1) and GC2F (also known as retGC-2), both of which are expressed in vertebrate rods and cones (8, 9). These specialized photoreceptor guanylate cyclases in outer segments of rods and cones resynthesize cGMP that is rapidly depleted through activated PDE upon light stimulus.

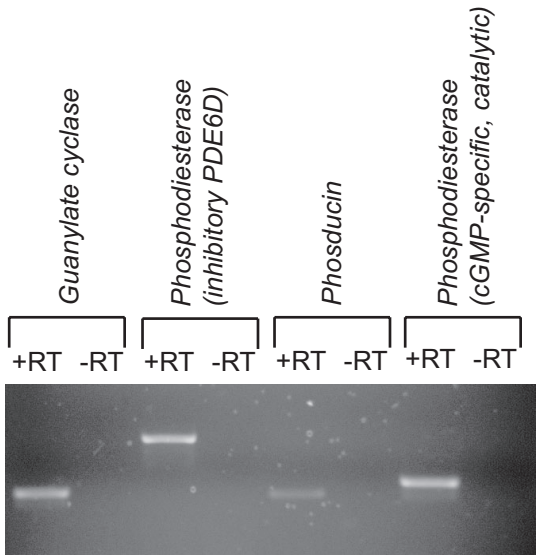

Fig. S3. Expression analysis of ciliary phototransduction cascade genes. RT-PCR analysis of *guanylate cyclase*, *phosphodiesterases*, and *phosducin* gene expression in rhopalia of *T. cystophora*. In all cases, no PCR product was obtained in the absence of reverse transcriptase (−RT).

A

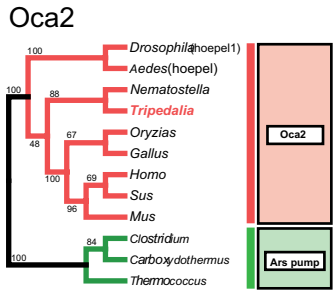

B

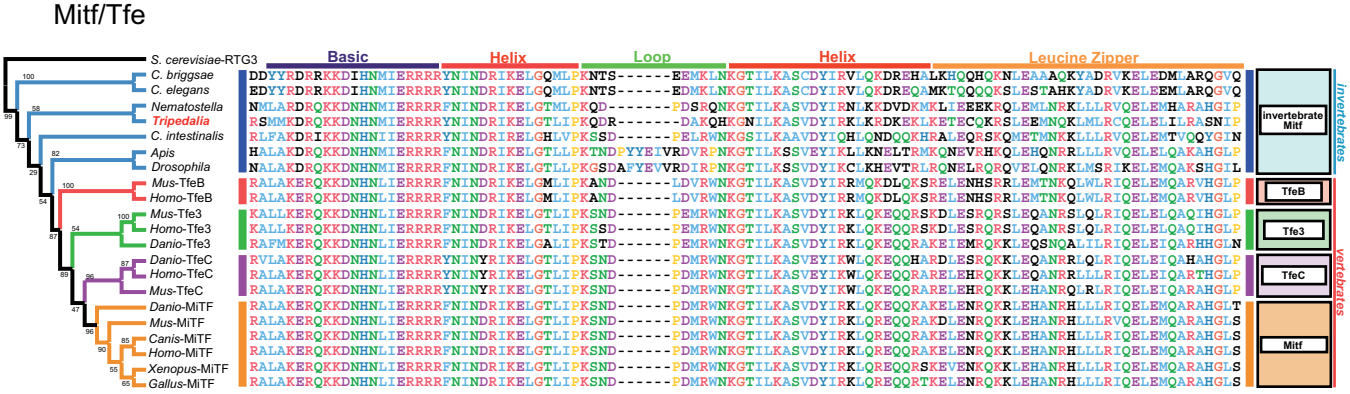

Fig. S4. Phylogenetic analysis of melanogenic pathway-specific genes. (*A*) Phylogenetic tree of the *Oca2* gene family. Oca2 proteins (also known as P protein, P permease, or hoepel) from different organisms and protein sequences of three arsenic pumps (closest homologues to Oca2 family) were aligned, and conserved transmembrane helices were used for phylogenetic analysis. The tree was inferred by the neighbor-joining method using arsenic pumps as outgroup sequences. The numbers above and under the branches indicate bootstrap support (1,000 replicates). (*B*) Alignment and phylogenetic tree of the *Mitf/TFE* gene family. The phylogenetic tree was inferred by the neighbor-joining method using *Saccharomyces cerevisiae* RTG3 as an outgroup sequence. Colored bars above the alignment demarcate the secondary structure motifs (according to ref. 10). *Caenorhabditis* sequences form an outgroup probably because of the high level of diversification.